

Terahertz pulse propagation through small apertures

Oleg Mitrofanov,^{a)} M. Lee, J. W. P. Hsu, L. N. Pfeiffer, K. W. West, and J. D. Wynn
Bell Laboratories, Lucent Technologies, 600 Mountain Avenue, Murray Hill, New Jersey 07974

J. F. Federici

Department of Physics, New Jersey Institute of Technology, Newark, New Jersey 07102

(Received 30 March 2001; accepted for publication 12 June 2001)

Transmission of single-cycle terahertz pulses through subwavelength apertures is experimentally studied in the near-field zone. Measurements of throughput for aperture sizes d as small as $\lambda/300$ show that the theoretical d^3 law requires a correction term which takes into account the physical thickness of the aperture screen. Frequency dependent transmission of the broad band pulses explains changes in their spectral and temporal characteristics. Practical application of small apertures in near-field microscope probes allows achievement of spatial resolution of $7 \mu\text{m}$ for pulses with a broad spectral content of $\lambda = 120\text{--}1500 \mu\text{m}$. © 2001 American Institute of Physics. [DOI: 10.1063/1.1392303]

The near-field imaging technique with an aperture-type probe is one of the methods to achieve high spatial resolution with free-space propagating terahertz (THz) pulses.^{1–5} Resolution of this method is defined by the aperture size. However, weak throughput of an aperture $d < \lambda/100$ in size limits its application. Electromagnetic waves also diffract onto small objects, such as apertures, resulting in significant changes in the THz pulse wave form.^{6,7} It is important to know for near-field image interpretation how the subwavelength aperture alters the spectral content and the temporal characteristics of the incident pulse.

It was demonstrated recently that the sensitivity of a near-field probe is significantly improved if a detecting element is placed in the near-field zone of the probe aperture.⁸ In this letter, we discuss THz pulse transmission through a subwavelength aperture in the near-field zone. We investigate the theoretical and practical limits of spatial resolution of the THz near-field imaging technique by studying the attenuation of the pulses transmitted through the aperture. The frequency dependent transmission is experimentally measured using THz time-domain spectroscopy. We show that the transmission process alters the pulse temporal wave form and spectrum, resulting in various effects such as pulse broadening, compression, time advancement, and a spectral blueshift. In application to near-field microscopy, we experimentally demonstrate spatial resolution of $7 \mu\text{m}$ using pulses with a spectral content of $\lambda = 120\text{--}1500 \mu\text{m}$.

In the experimental setup, the THz pulses are generated by a transient current in a photoconducting antenna.⁹ The THz radiation is collected and focused onto a square-shaped aperture by a system of parabolic mirrors and Si lenses [Fig. 1(a)]. The aperture is lithographically formed in a 600 nm thick gold screen on a GaAs surface. A $4 \mu\text{m}$ layer of GaAs separates the aperture from a detecting photoconducting antenna, which measures the electric field of the transmitted THz pulses in the near-field zone of the aperture [Fig. 1(b)]. We tested apertures ranging from $d = 5$ to $d = 50 \mu\text{m}$ (d is the square side). The cutoff frequency of the largest aperture

($d = 50 \mu\text{m}$) lies within the spectral bandwidth of the incident pulse, while the cutoffs of the smaller apertures ($d < 20 \mu\text{m}$) are significantly above the spectrum [Fig. 1(c)]. We measured the time-domain wave form of the transmitted THz pulse for every aperture. The incident THz pulse is measured using a similar setup without the gold screen. Using this information, we can extract transmission coefficients and phase shifts throughout the pulse spectrum.

The energy coupled into the aperture decreases as d decreases. The theory of transmission through small apertures in an infinitely thin metallic screen predicts the d^3 law for the electric field amplitude in the limit of $\lambda \gg d$.¹⁰ However, the thickness of the screen has to be taken into account in the case of real apertures. We approximate the aperture with an undersized waveguide model. For a wave with wave vector smaller than the cutoff, there is no propagating solution inside the waveguide. The wave tunnels through the waveguide, and the wave amplitude exponentially decreases with

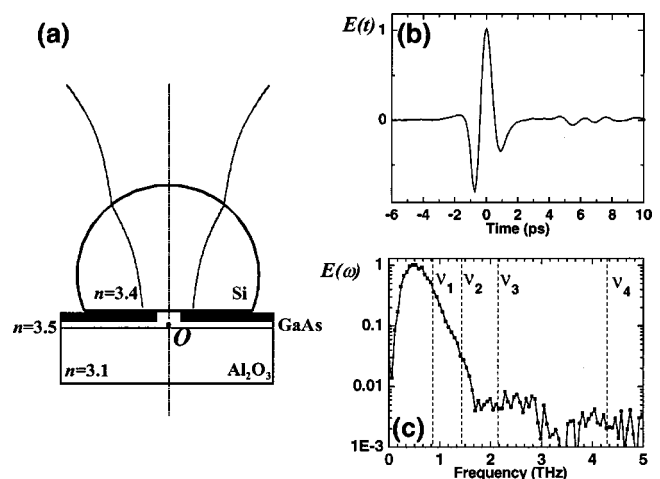


FIG. 1. (a) Schematic diagram of the experimental setup. The THz beam is focused onto the aperture with a Si hyperhemispherical lens, and the detecting dipole antenna on GaAs is placed at point O. (b) Waveform and (c) spectrum of the incident THz pulse. The dashed vertical lines show the cutoff frequencies of the apertures: ν_1 ($d = 50 \mu\text{m}$) = 0.86 THz, ν_2 ($30 \mu\text{m}$) = 1.43 THz, ν_3 ($20 \mu\text{m}$) = 2.14 THz, ν_4 ($10 \mu\text{m}$) = 4.49 THz, ν_5 ($5 \mu\text{m}$) = 8.57 THz.

^{a)}Electronic mail: olegm@lucent.com

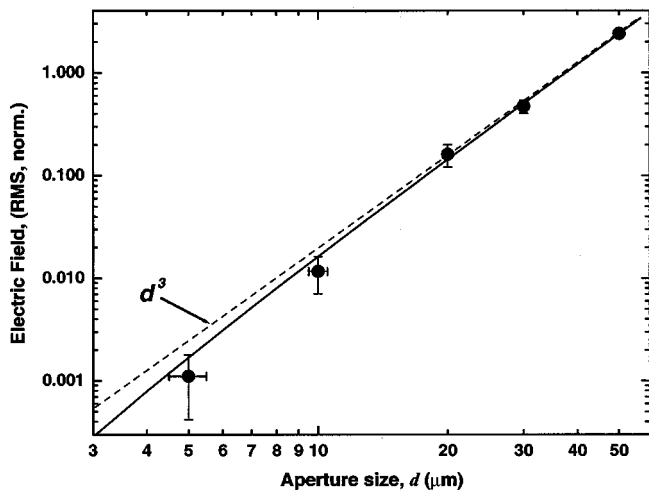


FIG. 2. Root mean square value of the electric field of the transmitted pulses ($\sqrt{\int |E(t)|^2 dt}$) (circles). The solid curve shows the d^3 law with the finite screen thickness correction.

the waveguide length. In the long wavelength limit ($\lambda \gg d$), the exponential term conveniently reduces to $\exp[-(\pi l/d)]$, where l is the screen thickness. The exponent is almost unity for relatively large apertures ($d \gg l$), for which the metallic screen can be assumed to be infinitely thin. The effect becomes significant when d becomes comparable to l . The transmission coefficient calculated using this model is shown in Fig. 2. The circles show the measured root mean square (rms) value of electric field of the THz pulses transmitted. The transmission function (in the limit of $\lambda \gg d$) has only implicit dependence on the wavelength through a constant scaling factor. The model explains sub- d^3 behavior of the amplitude within the measured range of aperture sizes, $d = 5 - 50 \mu\text{m}$.

The time-domain wave forms of the THz pulse transmitted through the apertures are shown in Fig. 3. The temporal pulse deformation is related to the high-pass properties of the subwavelength apertures. Spectral components above the cutoff frequency propagate through the aperture without significant change in amplitude, while the lower frequency components experience frequency dependent attenuation. The cutoff frequency of the $50 \mu\text{m}$ aperture is within the pulse bandwidth, and the transmitted pulse experiences significant deformation: the spectrum lacks the components below the cutoff (Fig. 4), and the pulse duration extends to ~ 5 ps [Fig. 3(b)]. As the aperture size decreases, more spectral components of the incident pulse fall into below the cutoff regime. For frequencies $\nu \ll \nu_c$, the variation of the transmission coefficient with frequency reduces and the aperture attenuates throughout the pulse spectrum with stronger suppression of the red end. As a result, the spectra of the pulses transmitted through the 5 and $10 \mu\text{m}$ apertures become flatter and the bandwidth effectively increases (Fig. 4). The pulse transmitted through the $5 \mu\text{m}$ aperture maintains its single-cycle characteristic and shows faster electric field oscillation than the incident pulse, corresponding to larger weight of the high frequency components.

If we apply the waveguide model, the phase shift that the wavelet experiences as it passes through the aperture consists of two parts: the phase shift associated with the wave coupling in and out of the aperture, and the phase delay due to

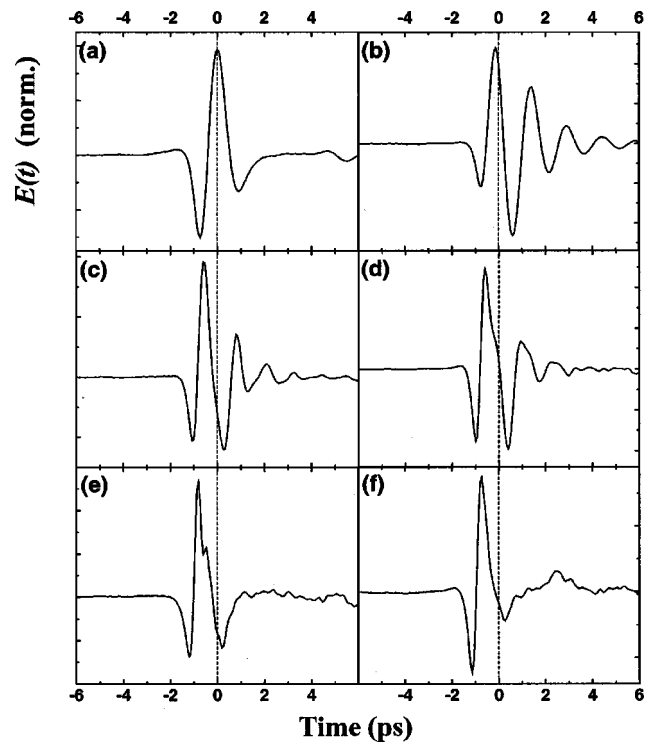


FIG. 3. Wave forms of (a) the incident pulse and the pulse transmitted through the apertures: $d =$ (b) 50 , (c) 30 , (d) 20 , (e) 10 , and (f) $5 \mu\text{m}$.

the waveguide. The second part is negligible since the screen thickness is small and the accumulated time delay is ~ 10 fs for propagating waves. The evanescent waves tunnel through the waveguide and experience no delay inside the waveguide. Therefore, we assume that the experimentally measured phase shift is due to aperture coupling. The inset of Fig. 4 shows the time shift as a function of frequency measured for the 5 and $50 \mu\text{m}$ apertures. The spectral components with frequencies larger than the cutoff frequency propagate through the aperture without any delay. Below the cutoff, however, there is a negative time delay, which corresponds to time advancement of the wavelet through a sub-

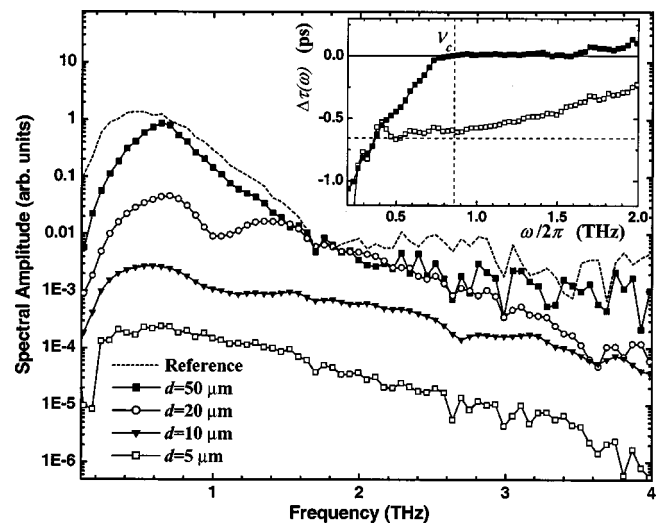


FIG. 4. Spectral content of the radiation transmitted through the apertures, and the frequency dependent time shift (inset). The dashed vertical line in the inset indicates the cutoff frequency of the $50 \mu\text{m}$ aperture, and the dashed horizontal line shows a time shift of -0.66 ps found for the center of gravity of the pulse transmitted through the $5 \mu\text{m}$ aperture.

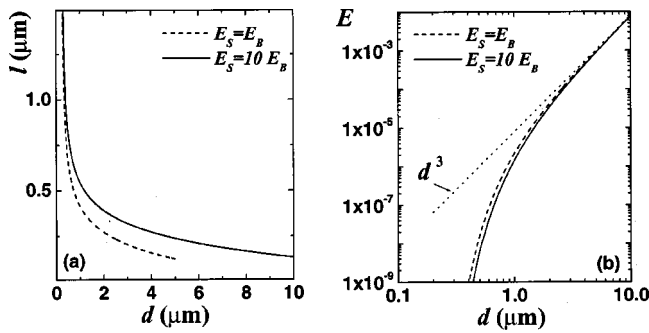


FIG. 5. (a) Required thickness of the aperture screen as a function of the aperture size and (b) the corresponding transmission coefficient for the THz pulse for two cases: the background (E_B) is on the same level as the signal (E_s) (dashed line) and the signal is 10 times larger than the background (solid line).

wavelength aperture. The center of the THz pulse incident on the $5 \mu\text{m}$ aperture appears on the other side ~ 0.66 ps earlier [Fig. 3(f)]. The negative time delay is attributed to regrouping of the spectral components of the pulse. In addition, an asymmetric wave form of the incident pulse contains faster oscillation in the pulse front. Given that higher frequencies suffer less attenuation, the leading part of the pulse is preferentially transmitted through the aperture while the slower varying tail of the pulse is suppressed. Note that the amplitude of the transmitted pulse is $\sim 10^{-4}$ of the incident pulse amplitude.

Temporal advancement of the peak of the THz pulse transmitted through a subwavelength aperture has been reported before; however, the center of gravity of the pulse was delayed in these experiments.¹¹ Our observation with the $5 \mu\text{m}$ aperture demonstrates that the center of gravity of the THz pulse [$t_c = \int |E(t)|^2 t dt / \int |E(t)|^2 dt$] can also experience temporal advancement in the transmission process. This effect can only be observed if the spectrum of the incident pulse does not contain significant energy in the components with frequencies above the cutoff.

A part of the incident power transmits through the metallic screen rather than through the aperture and reaches the detecting antenna, resulting in background. A 600 nm thick metallic (Au) screen attenuates the THz pulse to the level of $\sim 10^{-5} - 10^{-6}$, which is lower than the signal level (transmitted through the smallest of the apertures tested). However, an aperture smaller than $5 \mu\text{m}$ requires a thicker screen in order to maintain the signal at a higher level than the background. Using the d^3 law with the exponential correction term for the aperture transmission (Fig. 2) and the experimentally measured penetration depth of our Au films ($\delta = 50 \text{ nm}$), we can calculate the thickness of the Au screen required as a function of the aperture size. Figure 5(a) shows the screen thickness necessary to attenuate the incident THz

pulse to the level of the amplitude of the pulse transmitted through the aperture. The transmission functions corresponding to the required screen thickness are shown in Fig. 5(b). According to the model, the smallest aperture size that can be realized is $d \cong \pi \delta$ ($\sim 0.2 \mu\text{m}$). When this limit is approached, however, the effective size of the aperture is larger due to field penetration into metallic walls.

In application to near-field microscopy, we implement very small apertures in the near-field probes. The spatial resolution of such a probe is defined by the aperture size and is independent of the wavelength.¹² We measured resolution of $7 \mu\text{m}$ for the probe with the $5 \mu\text{m}$ aperture in the edge test with a 10%–90% criterion. In this experiment, an edge of a gold film deposited on a dielectric substrate is scanned at a distance of $\sim 1 - 2 \mu\text{m}$ over the probe aperture, and the amplitude of the THz pulse is measured.

In conclusion, we studied transmission of the THz pulses through apertures in the close to and far below the cutoff regimes. The transmission coefficient follows the d^3 law with the correction due to the screen thickness. The transmission process alters the temporal characteristics and spectral content of the THz pulses. The effects of temporal advancement through the aperture can be observed for particular pulse shapes. These results are general and independent of the aperture shape. In application to near-field microscopy, we explored the limit of spatial resolution and experimentally demonstrated $7 \mu\text{m}$ resolution for the range of wavelengths from 120 to $1500 \mu\text{m}$.

Two of the authors (O.M. and J.F.F.) gratefully acknowledge the support of the Army Research Office under Contract No. DAAD19-01-0009.

¹D. M. Mittleman, M. Gupta, R. Neelamani, R. G. Baraniuk, J. V. Rudd, and M. Koch, *Appl. Phys. B: Lasers Opt.* **68**, 1085 (1999).

²O. Mitrofanov, I. Brener, R. Harel, J. D. Wynn, L. N. Pfeiffer, K. W. West, and J. Federici, *Appl. Phys. Lett.* **77**, 3496 (2000).

³O. Mitrofanov, I. Brener, M. C. Wanke, R. R. Ruel, J. D. Wynn, A. J. Bruce, and J. Federici, *Appl. Phys. Lett.* **77**, 591 (2000).

⁴Q. Chen, Z. Jiang, G. X. Xu, and X.-C. Zhang, *Opt. Lett.* **25**, 1122 (2000).

⁵S. Hunsche, M. Koch, I. Brener, and M. C. Nuss, *Opt. Commun.* **150**, 22 (1998).

⁶A. Nahata and T. F. Heinz, *IEEE J. Sel. Top. Quantum Electron.* **2**, 701 (1996).

⁷J. Bromage, S. Radic, G. P. Agrawal, C. R. Stroud, Jr., P. M. Fauchet, and R. Sobolevski, *J. Opt. Soc. Am. B* **15**, 1399 (1998).

⁸O. Mitrofanov, R. Harel, M. Lee, L. N. Pfeiffer, K. West, J. D. Wynn, and J. Federici, *Appl. Phys. Lett.* **78**, 252 (2001).

⁹M. van Exter and D. R. Grischkowsky, *IEEE Trans. Microwave Theory Tech.* **38**, 1684 (1990).

¹⁰H. A. Bethe, *Phys. Rev.* **66**, 163 (1944); C. J. Bouwkamp, *Philips Res. Rep.* **5**, 321 (1950).

¹¹K. Wynne, J. J. Carey, J. Zawadzka, and D. A. Jaroszynski, *Opt. Commun.* **176**, 429 (2000).

¹²O. Mitrofanov, M. Lee, J. W. P. Hsu, I. Brener, R. Harel, J. Federici, J. D. Wynn, L. N. Pfeiffer, and K. W. West, *IEEE J. Sel. Top. Quantum Electron.* (submitted).